Evolution of Microstructure in the Liquid and Crystal Directions in a Quenched Block Copolymer Melt

N. P. Balsara,* B. A. Garetz,* and M. C. Newstein

Departments of Chemical Engineering, Chemistry, Materials Science, and Electrical Engineering, Polytechnic University, Six Metrotech Center, Brooklyn, New York 11201

B. J. Bauer and T. J. Prosa

Polymers Division, National Institute of Standards and Technology, Gaithersburg, Maryland 20899

Received June 17, 1998; Revised Manuscript Received August 31, 1998

ABSTRACT: The kinetics of the disorder-to-order transition in a polystyrene-*block*-polyisoprene copolymer was studied after it was thermally quenched from the disordered state to the ordered state. The ordered state consists of cylinders arranged on a hexagonal lattice. This state has liquid crystalline symmetry with liquidlike disorder along the cylinders axis and crystalline order in the hexagonal plane. We monitor the kinetics of microstructure formation in the liquid and crystalline directions by a combination of time-resolved depolarized light scattering and small-angle X-ray scattering experiments. At small quench depths, microstructure formation along the liquid and crystalline directions is strongly correlated during all stages of the disorder-to-order transition. We demonstrate that this is expected when microstructure formation occurs by classical nucleation and growth. At large quench depths, however, microstructure formation along the liquid and crystalline directions is not correlated. The growth of crystalline order occurs before the development of a coherent structure along the liquid direction. We argue that this may be a signature of spinodal decomposition in liquid crystals.

Introduction

The thermodynamic factors that govern the equilibrium properties of block copolymer melts are well understood.[1−4] Entropy dominates at high temperatures, leading to a homogeneous, disordered phase. Repulsive interactions between the blocks become increasingly important with decreasing temperature, and this leads to the formation of periodic, ordered phases with crystalline or liquid crystalline symmetry. Despite considerable efforts, many fundamental questions regarding the kinetics of disorder-to-order transitions remain unresolved.

Consider a block copolymer melt that is thermally quenched from the disordered state to the ordered state. It is conventional to describe the state of the system in terms of an order parameter that is zero in the disordered state and finite in the ordered state.[1] If the disordered phase is metastable with respect to the ordered phase then the phase transition will occur by nucleation and growth. In this case, the early stages of ordering would result in the formation of ordered droplets or grains in a continuum of disorder. The order parameter within isolated regions in the sample (grains) would have a nonzero equilibrium value, while the order parameter in the rest of the sample would be zero. With increasing time, the ordered grains grow by consuming the disordered phase. Theoretical descriptions of nucleation and growth in block copolymers have been proposed by Fredrickson and Binder[5] and Goveas and Milner.[6]

On the other hand, when the disordered phase is unstable with respect to the ordered phase, the phase transition will occur by spinodal decomposition. Theories for order formation by spinodal decomposition have been developed by Qi and Wang[7] and Laradji et al.[8] However, these theories are restricted to order−order transitions where the new ordered phase and the mother phase share an epitaxial relationship. We are not aware of any theories that address the nature of the transformation from disorder to order, when the disordered phase is unstable. In this case, certain Fourier modes of the concentration fluctuations that preexist in the disordered state will be amplified. The ordered phase develops throughout the sample, and the ordering kinetics consists of the growth of the amplitude of the order parameter. A schematic representation of the growth of ordered phases during nucleation and growth and spinodal decomposition in a block copolymer melt is shown in Figure 1. The ordered phase is represented by periodic concentration profiles, and the order parameter is proportional to the amplitude.

The location of the spinodal, i.e., the temperature (T) at which the mechanism of disorder-to-order changes from nucleation and growth to spinodal decomposition, remains a major unresolved issue. In the mean-field theory,[1] the spinodal temperature is located just below the stability limit of the cylindrical phase. Therefore, in this theory, the formation of cylindrical phases should occur by nucleation and growth for shallow quenches and by spinodal decomposition for deep quenches. On the other hand, the formation of lamellar phases is predicted to occur by spinodal decomposition because they are found deep in the microphase-separated region of the phase diagram.[1] Leibler anticipated that his theory would break down for perfectly symmetric block copolymers. Fredrickson and Helfand proposed a refined theory of block copolymer thermodynamics that accounts for the presence of fluctuations in the disordered state.[2] In this theory, the spinodal is suppressed to $T = 0$ K, implying that the formation of cylindrical and lamellar phases should occur by nucleation and growth, regardless of quench depth. The two widely accepted theories on block copolymer thermodynamics thus lead to dramatically different results with regard

10.1021/ma9809637 CCC: $15.00
Published on Web 10/14/1998

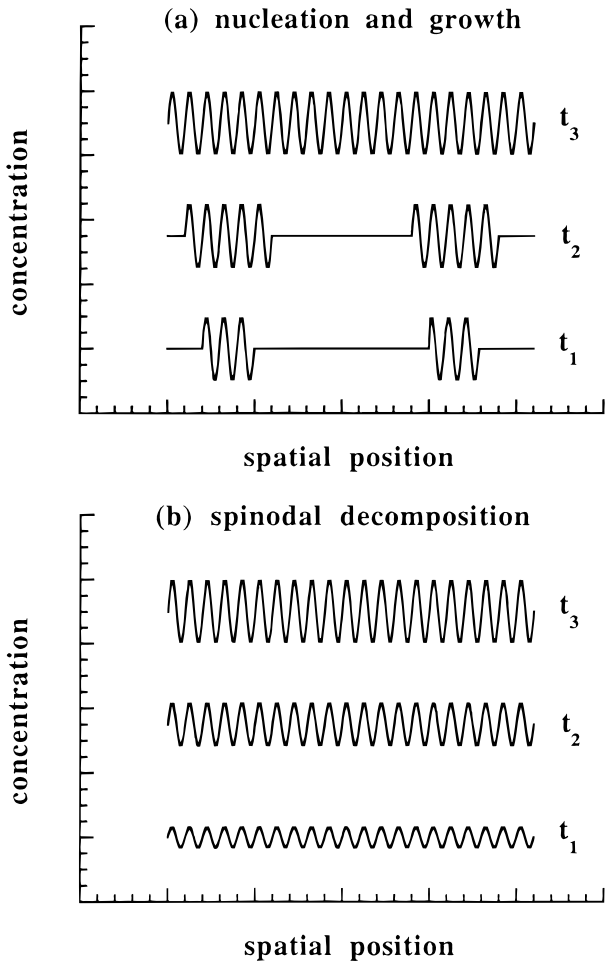

Figure 1. Schematic representation of the development of periodic concentration profiles by (a) nucleation and growth and (b) spinodal decomposition in a block copolymer melt as a function of time ($t_1 < t_2 < t_3$).

to the mechanism of the disorder-to-order transition.

Experimental studies of the kinetics of ordering transitions by time-resolved X-ray scattering were conducted by Harkless et al.,[9] Hashimoto et al.,[10] and Stuhn et al.[11] These experiments reveal the presence of two processes, a fast process that is believed to be related to the local segregation of the blocks and a slow process that leads to the development of long-range order. The question of phase transition mechanisms has been addressed by Hashimoto and Sakamoto,[12] Newstein et al.,[13−15] and Hajduk et al.[16] Unambiguous signatures of nucleation and growth were reported in refs 12−15. To our knowledge, unambiguous experimental signatures of spinodal decomposition have not yet been reported in block copolymer melts. An important first step was taken by Hajduk et al.[16] who found an abrupt change in the characteristics of the ordered structure as a function of quench depth. They suggested that this may be a signature of spinodal decomposition.

In this work we study the kinetics of the transformation of disorder to cylindrical order in a diblock copolymer melt. The cylindrical phase has liquid crystalline symmetry with liquidlike disorder along the cylinder axis and hexagonal order in the plane perpendicular to it. We use two independent methods to probe the growth of the liquid crystalline structure following a thermal quench from the disordered to the ordered state. The first probe is small-angle X-ray scattering (SAXS) wherein we follow the growth of the second-order Bragg reflection of the hexagonal structure (the $\sqrt{3}$ peak). This method thus focuses on the development of microstructure in the crystalline directions. The second probe is depolarized light scattering, wherein we exploit the fact that the ordered cylindrical grains are equivalent to uniaxial optical crystals with optic axes directed along the cylinder axes. The presence of hexagonal order is relatively unimportant. For example, grains composed of cylinders arranged on a cubic lattice would have the same optical anisotropy as conventional block copolymer cylinders arranged on a hexagonal lattice if the cylinder volume fraction and composition of the cylinders and matrix were identical.[17,18] The depolarized light scattering intensity is proportional to the volume of the coherently ordered grains. Thus, significant structural development along liquid *and* crystalline directions is necessary for obtaining measurable light scattering signals. The combined results of X-ray and light scattering experiments enable us to follow structural development along the liquid and crystalline directions during the disorder-to-order transition.

If we assume that grain growth proceeds by classical nucleation and growth, then the order parameter within the grain is at its equilibrium value during the entire growth process. In this case, microstructure formation along the liquid and crystalline directions must be strongly correlated. We find that this holds true for shallow quenches. For deeper quenches, however, we find that the small-angle X-ray scattering signal increases much more rapidly than the light scattering signal. This indicates that the development of the liquid and crystalline structures is not correlated. We propose that this may be a signature of spinodal decomposition in block copolymer melts.

Experimental Section

A polystyrene-*block*-polyisoprene copolymer was synthesized by high-vacuum anionic polymerization, as described in ref 19. The molecular masses of the polystyrene and polyisoprene blocks were 4 and 13 kg/mol, respectively, and we refer to this polymer as SI(4-13). The equilibrium properties of a melt of this polymer were obtained from high-resolution, X-ray scattering experiments.[20] The block copolymer forms an ordered phase consisting of polystyrene cylinders embedded in a polyisoprene matrix, arranged on a hexagonal lattice. The intercylinder spacing is 157 ± 11 Å and the cylinder radius is 40 ± 3 Å. The sample exhibits an disorder-to-order transition at 59 ± 1 °C. DSC scans at a heating rate of 10 °C/min were conducted on a fully ordered SI(4-13) melt. These measurements indicated that the glass transition temperature of the polystyrene microphase was near 50 °C, as described elsewhere.[19]

The block copolymer was disordered by heating to 70 °C and then cooled to predetermined temperatures in the ordered state. We present results for four quench temperatures: 56, 54, 52, and 50 °C. SAXS experiments were conducted at the National Institute of Standards and Technology in Gaithersburg, MD.[21−23] The 10 m SAXS facility, with pinhole collimation and a Cu Kα ($\lambda = 1.54$ Å) rotating anode source was used. A 1 mm thick sample was confined between Kapton windows. The depolarized light scattering experiments on SI(4-13) were conducted on an apparatus described in previous papers.[14,15] Previous experience indicated that the sample temperature was controlled to within ±0.2 °C during the ordering process. SAXS exposures were taken at 10 min intervals and averaged over 10 interval periods. Reported times, t, are taken as the center of the averaged time interval and rounded to the nearest minute.

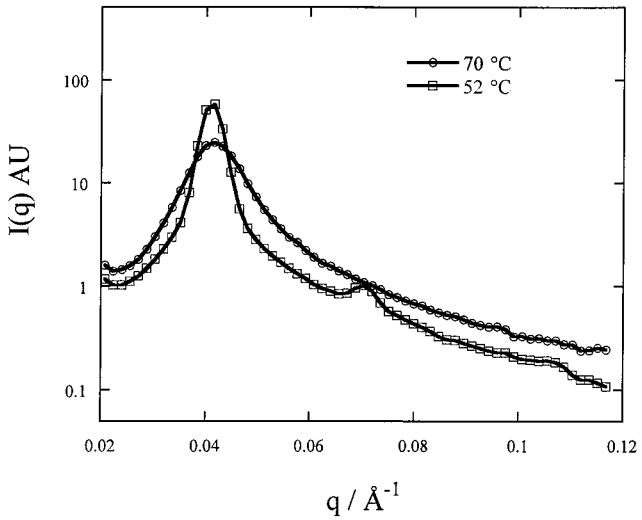

Figure 2. Typical small-angle X-ray scattering profiles from SI(4-13) in the disordered state (70 °C) and in the fully ordered state (52 °C at $t = 1400$ min). Relative errors are smaller than the symbols chosen to represent the data points.

Efforts were made to ensure that the samples were subjected to the same thermal history in the light scattering and X-ray scattering experiments. In both cases, the sample was quenched quiescently inside the temperature-controlled sample chamber and the time taken to reach the final temperature was about 20 min. Time zero ($t = 0$) is defined as the time at which the quench was initiated. We tried to reduce the time taken for the quench by shuttling the sample between two sample stages set to predetermined temperatures. However, we found that this led to irreproducible light scattering signals, indicating that the grain structure was affected by the physical movement of the sample. The sample temperature was controlled by measuring the temperature close to the sample but within the heating block. The relationship between this temperature and the sample temperature was established in separate experiments by inserting a thermocouple inside the sample. The temperatures used in the paper are nominal temperatures. The actual sample temperatures in the light scattering experiments were 55.5, 53.7, 52.0, and 50.0 °C, while the corresponding sample temperatures in the X-ray scattering experiments were 56.0, 54.0, 52.0, and 50.0 °C.

Results and Discussion

Typical SAXS data are shown in Figure 2 where we plot the scattering intensity, I_X, versus the scattering vector, q ($q = 4\pi \sin(\theta/2)/\lambda$, where θ is the scattering angle and $\lambda = 1.54$ Å is the wavelength of the incident X-rays). Data are obtained from the circular averaging of two-dimensional data files, and estimated uncertainties are calculated as the estimated standard deviation of the mean. In Figure 2 we show the scattering profile obtained before the quench at 70 °C and at $t = 1000$ min during the 52 °C quench. The scattering peak in the disordered state is due to the presence of concentration fluctuations.[1] The formation of the ordered phase results in the following qualitative changes in the SAXS profiles: the primary peak near $q_{max} \approx 0.04$ Å^{-1} sharpens and grows in height and a second-order peak emerges at $q = \sqrt{3}\, q_{max}$ Å^{-1}. The development of the second-order peak is clearly related to the development of hexagonal order. In contrast, the height and width of the primary peak may be related to the disordered fluctuations or the emerging ordered structure. For example, if there were an amplification of the concentration fluctuations without order formation, then one would detect an increase in the peak intensity. Thus, the increase in the scattering intensity at q_{max} is not necessarily an indication of order formation. However, the observed increase in the scattering intensity at q_{max} is accompanied by a distinct narrowing of the primary peak (Figure 2). Consequently, the scattering intensity on either side of q_{max} decreases with time. If the increase in the scattering intensity at q_{max} were due to the amplification of concentration fluctuations then the scattering intensity on either side of the peak would also increase with time.[1,2,19,20] The decrease in SAXS intensity in the wings of q_{max} is another clear signature of the ordering process.

The scattering profiles obtained at 50, 54, and 56 °C were very similar to those shown in Figure 2. In Figure 3a−c we present the time evolution of various SAXS features as a function of quench depth. In Figure 3a we show the time dependence of the primary peak intensity, I_{max}. In Figure 3b we show the time dependence of the primary peak width at half-height, $w_{1/2}$. In Figure 3c we show the time dependence of the integrated area under the second-order peak, I_2. These parameters were obtained by fitting the scattering profile in the vicinity of the scattering peaks to a single Gaussian peak with a linear background. A nonlinear least squares algorithm was employed to return the peak maximum, peak position, peak width, baseline, and peak areas, with appropriate estimates of error. Error bars in plots represent the standard deviation of the goodness of fit.

The values of I_{max}, $w_{1/2}$, and I_2 obtained at long times ($t = 800$ min) are independent of sample temperature in the 50−56 °C range (Figure 3a−c). This implies that the microstructures obtained in the fully ordered sample at different quench depths cannot be distinguished by SAXS. However, as shown in Figure 3a−c, the time dependence of I_{max}, $w_{1/2}$, and I_2 are strong functions of quench depth. Thus, differences in the kinetics of the phase transition can be studied by analysis of the SAXS data.

The time dependence of I_{max} and I_2 are qualitatively similar. At small quench depths (56 and 54 °C), the values of I_{max} and I_2 during the first 200 min are nearly independent of time, indicating undetectable structural changes. We refer to this as the induction regime. This regime is followed by a regime of rapid ordering that lasts for about 800 min. During this time significant changes in I_{max} and I_2 were recorded. At longer times, I_{max} and I_2 become time-independent again, indicating the completion of the ordering process. At higher quench depths (52 and 50 °C), however, the ordering kinetics are rapid in the first 400 min, as seen in Figure 3a−c. The induction regimes found at 54 and 56 °C are no longer evident at these temperatures. There thus appears to be an abrupt change in the SAXS signatures of the ordering kinetics, when the quench temperature is changed from 54 to 52 °C.

For a given quench, I_2 is a direct measure of the development of crystalline order in the sample. If we assume that the equilibration of the local order parameter is extremely rapid, then I_2 is proportional to the volume fraction of material with hexagonal order. It is evident that regardless of quench temperature, the value of I_2, at long times, approaches about 0.0012. If we assume that the entire sample is filled with ordered grains at long times, then $I_2/0.0012$ is an estimate of the volume fraction of the hexagonal phase. We use the symbol ϕ_X to denote this quantity, which represents the

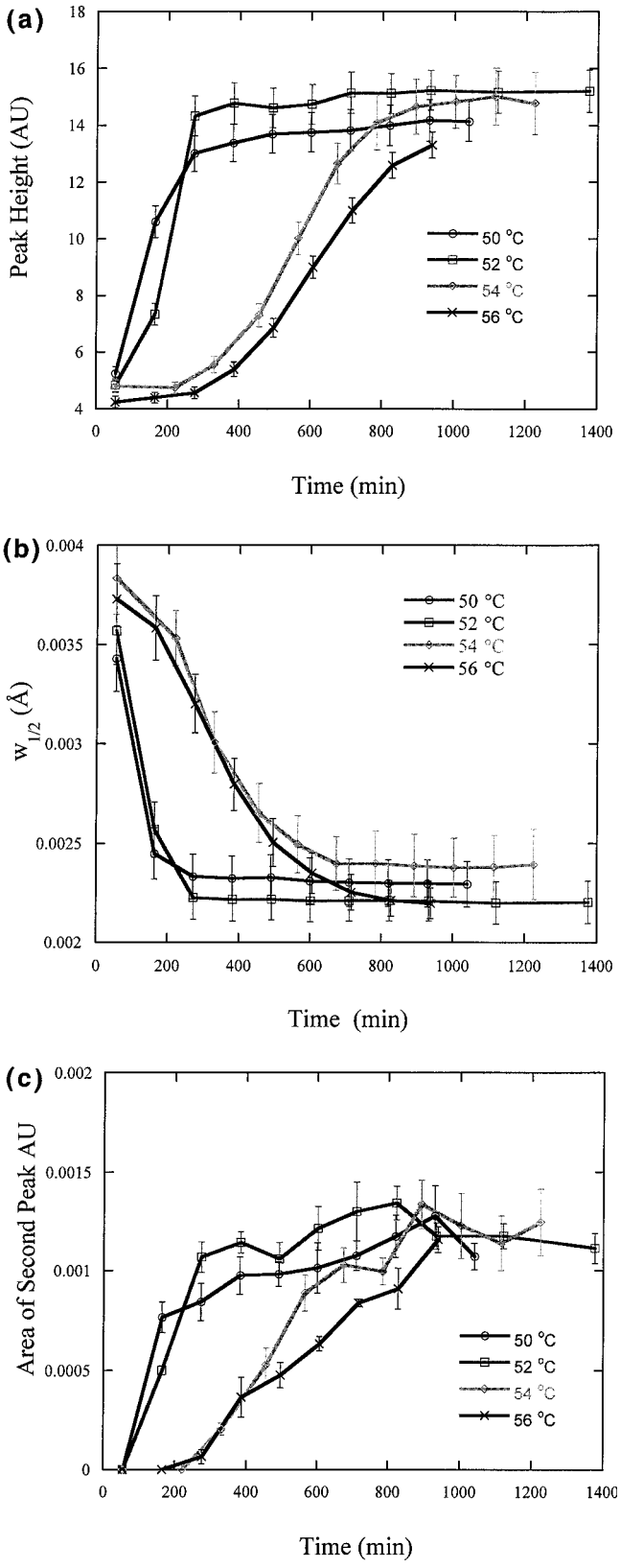

Figure 3. Time dependence of the signatures of order formation: (a) primary peak height, I_{max}; (b) primary peak width at half-maximum, $w_{1/2}$; (c) area under second-order peak, I_2. Error bars signify 1 σ relative uncertainties.

ordered phase volume fraction as determined by X-ray scattering.

Typical depolarized light scattering results are shown in Figure 4a, where we show the time dependence of the depolarized light scattering profile $I(q)$ [the definition of q is identical to that used in the discussion of the SAXS data, $q = 4\pi \sin(\theta/2)/\lambda$, where θ is the scattering angle and $\lambda = 0.532$ μm is the wavelength of the incident light] along the polarizer/analyzer axes for the 52 °C quench. Additional details regarding the light scattering data and their analysis are given in ref 15. The data labeled $t = 0$ min in Figure 4 refer to the measured scattering from the disordered state, prior to the quench, and are probably due to imperfections in our scattering apparatus; we consider this to be background noise. To obtain information about the ordered state, we subtract this signal from that obtained during the ordering process. During very early times ($t \leq 180$ min), the measured signal is comparable to that obtained from the disordered sample and hence this subtraction leads to erratic results. However, at longer times ($t \geq 240$ min), the scattering signal is 1 order of magnitude greater than the background, and uncertainties in the background are no longer an issue. The scattering intensity continues to increase with increasing time and saturates at about $t = 900$ min. This indicates the completion of the disorder-to-order transition.[14,15]

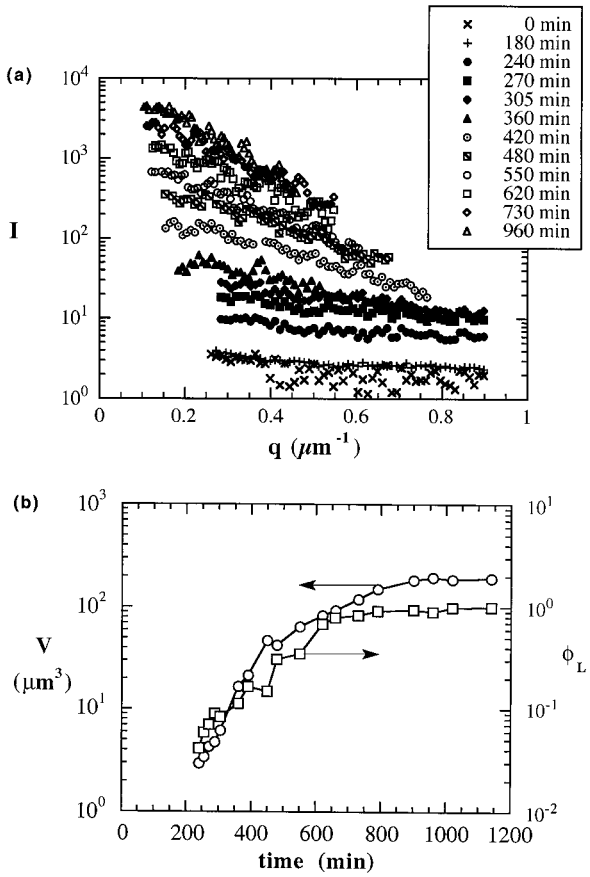

Figure 4. (a) Typical depolarized light scattering from SI(4-13). Time dependence of the scattered light along the polarizer/analyzer axes at 52 °C. Clear evidence for ordering is seen at times greater than or equal to 240 min. (b) The time dependence of average grain volume, V, and fraction of sample volume occupied by the ordered phase, as determined by light scattering, ϕ_L. The relative errors in V and ϕ_L are less than 10% and 5%, respectively.

In this paper we are mainly interested in computing the time dependence of the volume fraction of the ordered phase, so that we can make direct comparisons with the X-ray scattering data. The volume fraction of the ordered phase can be estimated from the forward

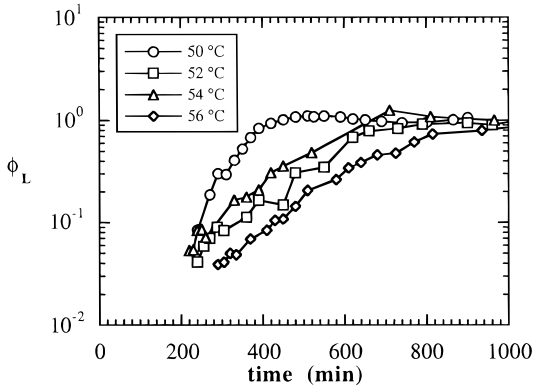

Figure 5. Time dependence of ϕ_L, the volume fraction of ordered grains determined by depolarized light scattering. The relative uncertainties are less than 5%.

depolarized light scattering intensity (i.e., as $q \rightarrow 0$), provided the time dependence of the order parameter within the grains and the size and shape of the grains is known. The average grain volume, V, grain shapes, and the nature of intergrain correlations are determined from the angular spread of the scattered light (Figure 4a); see ref 15 for more details. We make additional assumptions that (1) the order parameter within the grains is time independent and (2) the volume fraction of the ordered phase is unity at long times. The first assumption is consistent with classical nucleation and growth theory that the order parameter within the grains is at its equilibrium value at all times, while the second assumption is identical to that used in the analysis of the X-ray scattering data.

The time dependence of the average grain volume (V) and the volume fraction (ϕ_L) occupied by grains, determined by light scattering, for the 52 °C quench is shown in Figure 4b. It is evident that $V(t)$ and $\phi_L(t)$ are more or less parallel to each other, implying that the increase in the volume fraction of the ordered phase is primarily due to the growth of existing grains; see refs 14 and 15 for details. The trends for $V(t)$ and $\phi_L(t)$ at other quench depths were similar to those reported in Figure 4b for the 52 °C quench.[15] Fits of the data typically give standard deviations of ±10% in $V(t)$ and ±5% in $\phi_L(t)$.

The time dependence of the volume fraction of ordered grains determined by light scattering for each of the four quenches is shown in Figure 5. At all temperatures, we find that grain growth occurs in three stages: an induction stage where the light scattering patterns are indistinguishable from those obtained in the disordered state, an early stage of grain growth where rapid changes in the light scattering profiles are recorded, followed by a regime of slow (or undetectable) grain growth. The characteristic length of the grains along the cylinder axis and perpendicular to it may be different due to the anisotropic nature of the ordered grains.[14,15] Let l be the characteristic length of the grains along the optic axis, and w, the characteristic length of the grains perpendicular to the optic axis. The characteristic size of the grains, when the measured light scattering signal is distinctly greater than that obtained in the disordered state, ranges between 1 and 2 μm, regardless of quench depth.[15] For example, at 52 °C this occurs at $t = 240$ min (see Figure 4). We therefore conclude that our light scattering apparatus is insensitive to the presence of ordered grains if their length scale is less than 1 μm. This is by no means an intrinsic limitation of depolarized light scattering. It

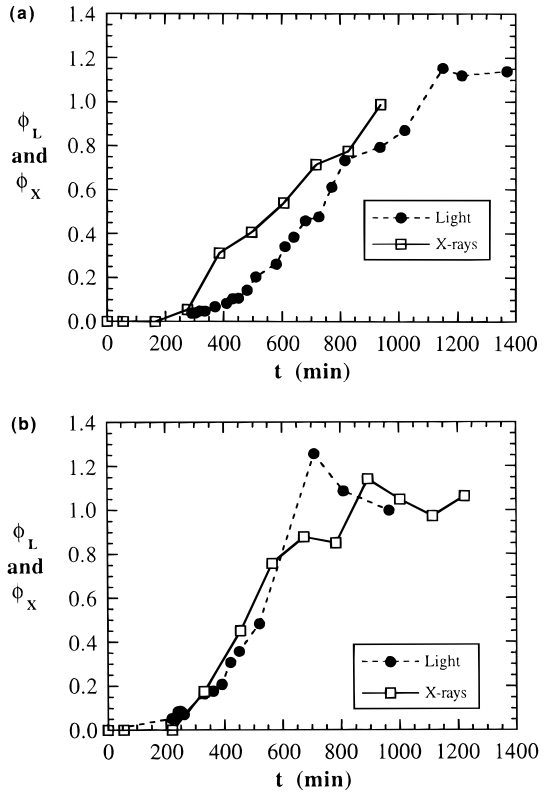

Figure 6. Comparison of the volume fraction of ordered grains determined by depolarized light scattering [$\phi_L(t)$] and small angle X-ray scattering [$\phi_X(t)$]: (a) 56 °C; (b) 54 °C.

merely reflects the limitations of the particular apparatus that we have built and the relatively small optical anisotropy and scattering power of the ordered grains that we wish to detect. Note that the scattered intensity is proportional to lw^2. The light scattering signal is thus negligible if either l *or* w is much smaller than the detection limit. Our light scattering apparatus is thus incapable of distinguishing between liquidlike disorder obtained above 59 °C and ordered structures with l or w significantly less than 1 μm.

In Figure 6a,b, we compare the ordering kinetics as probed by light and X-ray scattering by plotting the time dependence of ϕ_L and ϕ_X at 56 °C (Figure 6a) and 54 °C (Figure 6b). It is evident that the increase in the volume fraction of the crystal structure, detected by X-ray scattering, is in good agreement with the increase in the volume fraction of ordered grains, detected by light scattering. Note that the two methods used to estimate the volume fraction of the ordered phase are entirely independent. SAXS is sensitive to the formation of a hexagonal structure with a length scale of 0.015 μm, while light scattering is sensitive to the formation of ordered grains with length scales of 1 μm or larger. The characteristic lengths that are probed by the two techniques thus differ by 2 orders of magnitude. In addition, the source of the scattering signals in the two experiments are entirely different. SAXS depends on electron density contrast between the cylinders and the matrix, while depolarized light scattering depends on the optical anisotropy of the ordered grains relative to the surrounding medium. Despite these difference, the agreement between ϕ_L and ϕ_X is nearly quantitative at 56 and 54 °C. This agreement provides strong evidence for the fact that the mechanism for the disorder-to-order transition is classical nucleation and growth. Our analysis of the SAXS and light scattering data are based

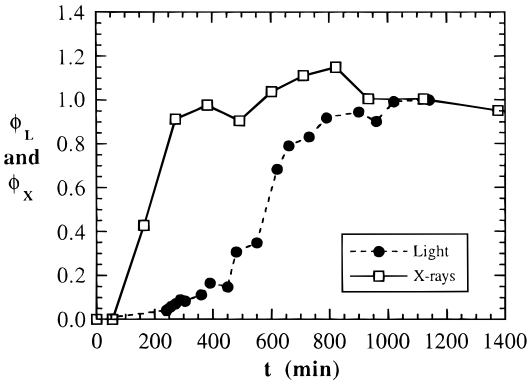

Figure 7. Comparison of the volume fraction of ordered grains determined by depolarized light scattering [$\phi_L(t)$] and small angle X-ray scattering [$\phi_X(t)$] at 52 °C.

on the assumption that the disorder-to-order transition occurs by nucleation and growth. Subtle deviations from classical nucleation and growth would cause deviations between ϕ_L and ϕ_X. For example, if the order within the grains became better defined with increasing time, then this would affect ϕ_L and ϕ_X differently, and this would lead to deviations between ϕ_L and ϕ_X at a given time. It is also worth noting that the quench was performed in different sample chambers. Past experience has shown that ordering kinetics and grain structure are sensitive to small changes in thermal history and annealing temperature.[13−15] The agreement between ϕ_L and ϕ_X at 54 and 56 °C suggests that the unavoidable differences in the thermal history of the sample in the SAXS and light scattering apparatuses do not affect the kinetics of the disorder-to-order transition.

In Figure 7 we compare the time dependence of ϕ_L and ϕ_X at 52 °C. It is evident that there is a substantial difference between ϕ_L and ϕ_X at a given time. For example, at $t = 300$ min, ϕ_X is 0.9, while ϕ_L is only 0.05. In other words, when 90% of the sample is occupied by the hexagonal phase, the volume fraction of ordered grains detected by light scattering is only about 5%. Similar disagreement is seen at 50 °C; at $t = 250$ min, $\phi_X = 0.7$ while $\phi_L = 0.08$ (see Figures (3c and 5)). It is evident that at the deeper quenches (52 and 50 °C), the rate of growth of the hexagonal phase, detected by X-ray scattering, occurs much more rapidly than the rate of growth of the ordered grains detected by light scattering.

We propose that the substantial difference between $\phi_L(t)$ and $\phi_X(t)$ at 52 and 50 °C is due to the fact that the two techniques probe different aspects of the liquid crystalline microstructure. At a temperature of 52 °C and $t = 300$ min, the sample is filled (or nearly so) with hexagonal order but there is no evidence of micron-sized grains. A microstructure that is consistent with these observations is shown schematically in Figure 8a. This is in contrast to the expected microstructure within classical nuclei, shown in Figure 8b. In Figure 8a we show an array of hexagonally packed, wormlike cylinders with a limited persistence length. Consider a system where the persistence length of the cylindrical domains and the coherence length of the microstructure in the crystal directions are both less than 1 μm. If such a structures occupied 90% of the sample at $T = 52$ °C and $t = 300$ min, then the resulting SAXS and light scattering data would be consistent with that presented in Figure 7. However, the wormlike cylinders are not

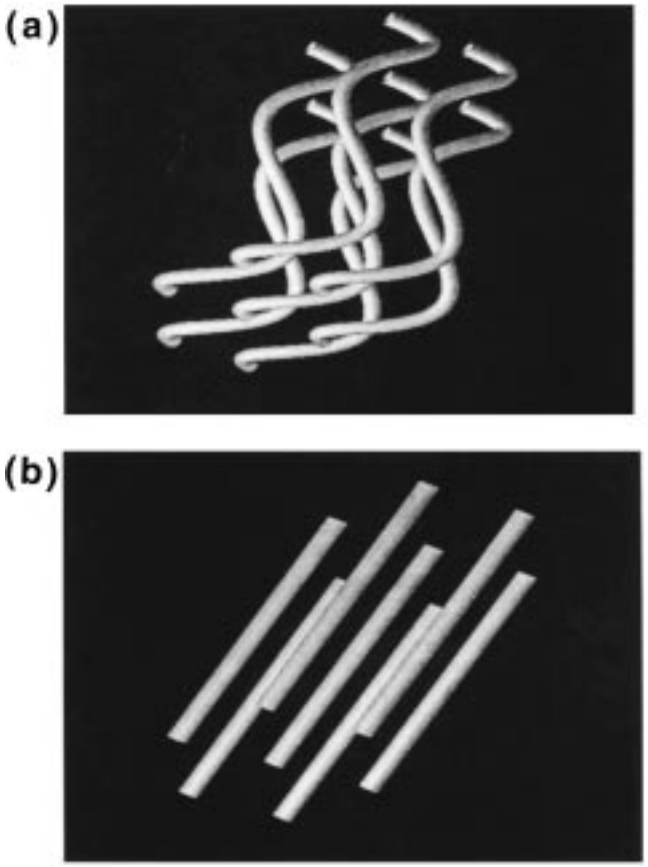

Figure 8. Schematic view of the cylindrical ordered phase formed during the early stage of order formation at temperatures (a) below 53 °C and (b) above 53 °C.

stable and eventually the cylinders must straighten. At 52 °C this straightening process begins at $t \approx 250$ min and is completed by $t \approx 600$ min. It is evident that the growth processes at (52 and 50) °C are very different from classical nucleation and growth. We therefore consider the possibility that the phase transition mechanism for the disorder-to-order transition at these temperatures may be spinodal decomposition.

The instantaneous structure of a spinodally decomposed binary liquid mixture is well-established. The structure is isotropic, and it can be constructed by superposing sinusoidal concentration profiles with random phase and direction but fixed wavelength λ_{max}.[24] The random phase and direction are due to the fact that the structural development in different parts of the sample occurs incoherently. The fixed wavelength defines the periodicity of the structure, which, in Fourier space, is represented by a maximum within a spherical shell of wave vectors centered around $q_{max} = 2\pi/\lambda_{max}$.

The situation is somewhat different in block copolymer melts. The disordered state in the vicinity of the order-to-disorder transition (ODT) has many of the characteristics of a spinodally decomposed binary blend. The Fourier space representation of the disordered structure consists of a maximum within a spherical shell. Quenching the material into the spinodal region will result in the amplification of wave vectors in specific directions, corresponding to the symmetry of the crystalline directions of cylindrical phase. However, in analogy to the binary blend case, the hexagonal structure will emerge incoherently throughout the sample, due to the instability of the disordered phase. It is evident that such a process will, in fact, lead to a

structure that is depicted schematically in Figure 8a.

We thus see that the rapid propagation of order by spinodal decomposition in SI(4-13) leads to a highly disorganized cylindrical mesophase with coherent order being restricted to length scales that are much smaller than 1 μm. At 52 °C this process takes about 250 min (Figure 3c) and is analogous to the initial stages of spinodal decomposition, as described by Cahn.[24] The processes that follow (t > 250 min at T = 52 °C) are analogous to the coarsening processes that occur during the intermediate and late stages of spinodal decomposition. In binary fluids, the early stages of spinodal decomposition lead to a bicontinuous structure with a large interfacial area per unit volume. The interfaces can be regarded as high free energy defects, and the subsequent coarsening processes lead to the elimination of these defects.[25] In the case of cylindrical block copolymers, the defects are topological in nature and can be either continuous (texture) or discrete (points, lines, and walls). We do not know the precise nature of defect structures in block copolymers with cylindrical microstructure, particularly during the early stages of the transformation from disorder-to-order. Hence, for simplicity, we have only shown continuous defects in Figure 8a. In fact we expect to find a wide variety of defects in the poorly ordered material that forms during the early stages of spinodal decomposition. The light scattering data at 52 °C, shown in Figure 4b, indicate that well-ordered grains grow by consuming the surrounding poorly ordered regions. Perhaps, the statistics of spinodal decomposition in block copolymers are such that at the end of the ordering process, a few regions are better organized than others. These regions act as nuclei for the subsequent growth of coherently ordered, micron-sized grains. The late stages of order formation at large quench depths (e.g., t > 250 min at 52 °C) may thus resemble nucleation and growth.[26]

Concluding Remarks

The evolution from disorder-to-order in a block copolymer melt has been studied by small-angle X-ray scattering and depolarized light scattering. At small quench depths ($T_{ODT} - T$ < 6 K, where T is the tempering temperature and T_{ODT} is the order-to-disorder transition temperature) we find strong evidence for nucleation and growth. In this regime, the increase in the light scattering and X-ray scattering signals are strongly correlated. Conversely, at large quench depths ($T_{ODT} - T$ > 6 K), the X-ray scattering signal increases much more rapidly than the light scattering signal. We propose that this may be a signature of spinodal decomposition. The temperature dependence of the Flory−Huggins interaction parameter, χ, in SI(4-13) was estimated from neutron scattering measurements in the disordered state.[19,26] The following expression was obtained

$$\chi = -0.27 + 43.8/T \qquad (1)$$

on the basis of a reference volume of 150.3 Å^3. This implies that the ratio χ_{ODT}/χ_S, where χ_S is the value of χ at the spinodal (spinodal temperature is taken to be 326 K) and χ_{ODT} is the value of χ at the disorder-to-cylinder transition, determined in SI(4-13) is 0.977.

In a related paper, Hajduk et al. studied the mechanism of the ordering transition in a poly(ethylene-*co*-propylene)-*block*-polyethyethylene-*block*-poly(ethylene-*co*-propylene) copolymer and observed qualitative changes in the coherence of the ordered state as a function of quench depth.[16] Their data suggest that at quench depths greater than 18 °C, the coherence of the ordered structure was substantially lower than that obtained at lower quench depths. They postulated two alternative interpretations for this observation: (1) the nucleation barrier at the higher quench depths is much less than kT, so that nucleation of the ordered phase occurs rapidly throughout the sample, or (2) the stability limit of the disordered phase was reached and the sample underwent spinodal decomposition. Binder and coworkers have shown theoretically that the crossover from nucleation and growth to spinodal decomposition in binary blends is smooth.[27] This implies that even in relatively well-studied systems such as binary blends, one cannot make a clean distinction between rapid homogeneous nucleation with nucleation barriers less than kT and spinodal decomposition. Perhaps the same will hold for ordering transitions in liquid crystals; i.e., the boundary between nucleation and growth and spinodal decomposition is not sharp. Using the published expression of χ for poly(ethylene-*co*-propylene)/polyethyethylene interactions,[28] and using the second interpretation, the data of Hajduk et al. give χ_{ODT}/χ_S = 0.961. This is very close to 0.977, the value that we have obtained in SI(4-13).

If the analogy between block copolymers and binary blends holds, then the true signatures of spinodal decomposition can only be established when the quenches are performed in the regime where χ is significantly greater than χ_S; i.e., the experiments are done in a region well removed from the estimated crossover from nucleation and growth to spinodal decomposition. Of course, the ordering kinetics in this regime will be rapid due to the large thermodynamic driving forces, and time-resolved measurements will therefore be challenging. Efforts to design new experiments that will enable us to meet these challenges are underway.

Acknowledgment. This paper owes much to stimulating and educational discussions with Frank Bates on the subject of phase transition mechanisms in block copolymers. We thank John Barnes for use of the NIST SAXS facility and data reduction software and H. J. Dai and M. Y. Chang for the acquisition and analysis of the light scattering data. Financial support from the National Science Foundation (DMR-9457950) and Research Corp. is gratefully acknowledged. Acknowledgment is made to the donors of the Petroleum Research Fund, administered by the American Chemical Society, for support of this research.

References and Notes

(1) Leibler, L. *Macromolecules* **1980**, *13*, 1602.
(2) Fredrickson, G. H.; Helfand, E. *J. Chem. Phys.* **1987**, *87*, 697.
(3) Bates, F. S.; Schulz, M. F.; Khandpur, A. K.; Forster, S.; Rosedale, J. H.; Almdal, K.; Mortensen, K. *Faraday Discuss.* **1994**, 98, 7.
(4) Hajduk, D. A.; Takenouchi, H.; Hillmyer, M. A.; Bates, F. S.; Vigild, M. E.; Almdal, K. *Macromolecules* **1997**, *30*, 3788.
(5) Fredrickson, G. H.; Binder, K. *J. Chem. Phys.* **1989**, *91*, 7265.
(6) Goveas, J. L.; Milner, S. T. *Macromolecules* **1997**, *30*, 2605.
(7) Qi, S.; Wang, Z. G. *Phys. Rev. Lett.* **1996**, *76*, 1679.
(8) Laradji, M.; Shi, A. C.; Noolandi, J.; Desai, R. C. *Macromolecules* **1997**, *30*, 3242.
(9) Harkless, C. R.; Singh, M. A.; Nagler, S. E.; Stephenson, G. B.; Jordan-Sweet, J. L. *Phys. Rev. Lett.* **1990**, *64*, 2285.
(10) Hashimoto, T.; Kowsaka, K.; Shibayama, M.; Suehiro, S. *Macromolecules* **1986**, *19*, 754.

(11) Stuhn, B.; Vilesov, A.; Zachmann, H. G. *Macromolecules* **1994**, *27*, 3560.
(12) Hashimoto, T.; Sakamoto, N. *Macromolecules* **1995**, *28*, 2329.
(13) Newstein, M. C.; Garetz, B. A.; Dai, H. J.; Balsara, N. P. *Macromolecules* **1995**, *28*, 4587.
(14) Dai, H. J.; Balsara, N. P.; Garetz, B. A.; Newstein, M. C. *Phys. Rev. Lett.* **1996**, *77*, 3677.
(15) Newstein, M. C.; Garetz, B. A.; Balsara, N. P.; Chang, M. Y.; Dai, H. J. *Macromolecules* **1998**, *31*, 64.
(16) Hajduk, D. A.; Tepe, T.; Takenouchi, H.; Tirrell, M.; Bates, F. S.; Almdal, K.; Mortensen, K. *J. Chem. Phys.* **1998**, *106*, 326.
(17) Fowles, G. R. *Introduction to Modern Optics*; Dover: New York, 1975.
(18) Born, M.; Wolf, E. *Principles of Optics*; Pergamon: Oxford, U.K., 1975.
(19) Lin, C. C.; Jonnalagadda, S. V.; Kesani, P. K.; Dai, H. J.; Balsara, N. P. *Macromolecules* **1994**, *27*, 7769.
(20) Perahia, D.; Vacca, G.; Patel, S. S.; Dai, H. J.; Balsara, N. P. *Macromolecules* **1994**, *27*, 7645.
(21) Barnes, J. D.; Mopsik, F. *Ann. Technical Conf. Proc., Soc. Plast. Eng.* **1988**, *12*, 1179.
(22) Hendricks, R. W. *J. Appl. Crystallogr.* **1978**, *11*, 15.
(23) Certain equipment and instruments or materials are identified in this paper in order to adequately specify the experimental details. Such identification does not imply recommendation by the National Institute of Standards and Technology nor does it imply the materials are necessarily the best available for the purpose.
(24) Cahn, J. W. *Trans. Metall. Soc. AIME* **1967**, *242*, 166.
(25) Ohta, T.; Jasnow, D.; Kawasaki, K. *Phys. Rev. Lett.* **1982**, *49*, 1223.
(26) Balsara, N. P.; Garetz, B. A.; Chang, M. Y.; Dai, H. J.; Newstein, M. C.; Goveas, J. L.; Krishnamoorti, R.; Rai, S. *Macromolecules* **1998**, *31*, 5309.
(27) Binder K.; Stauffer, D. *Adv. Phys.* **1976**, *25*, 343.
(28) Bates, F. S.; Rosedale, J. H.; Fredrickson, G. H. *J. Chem. Phys.* **1990**, *92*, 6255.

MA9809637